Griffiths-Wheeler geometrical picture of critical phenomena: Experimental testing for liquid-liquid critical points

Jacobo Troncoso, Diego González-Salgado, Claudio A. Cerdeiriña, Enrique Carballo, and Luis Romaní
Departamento de Física Aplicada, Facultad de Ciencias de Ourense, Universidad de Vigo, Campus As Lagoas 32004 Ourense, Spain
(Received 13 July 2004; revised manuscript received 13 October 2004; published 24 February 2005)

An experimental approach to the verification of specific relations between thermodynamic properties as predicted from the Griffiths-Wheeler theory of critical phenomena in multicomponent systems is developed for the particular case of ordinary liquid-liquid critical points of binary mixtures. Densities $\rho(T)$, isobaric heat capacities per unit volume $C_p(T)$, and previously reported values of the slope of the critical line $(dT/dp)_c$ for five critical mixtures are used to check the thermodynamic consistency of C_p and ρ near the critical point. An appropriate treatment of $\rho(T)$ data is found to provide the key solution to this issue. In addition, various alternative treatments for $C_p(T)$ data provide values for both the critical exponent α and the ratio between the critical amplitudes of the heat capacity A^+/A^- that are in agreement with their widely accepted counterparts, whereas two-scale-factor universality is successfully verified in one of the systems studied.

DOI: 10.1103/PhysRevE.71.021503 PACS number(s): 64.70.Ja, 64.60.Fr, 05.70.Jk

I. INTRODUCTION

Improvements in experimental techniques during the 1960s stimulated an increasing interest in the study of the criticality of fluids and led to the conclusion that the anomalies in thermodynamic and transport properties near critical points were governed by power laws with critical exponents that departed significantly from those predicted by "classical" mean-field theories. This goal was the starting point for the development of the modern theory of critical phenomena, which, among other important contributions, was dramatically advanced by the establishment of the scaling and universality hypotheses, and the formulation of the renormalization group theory [1]. Current research on criticality of fluids is mainly focused on complex fluids such as polymer, micellar, and ionic solutions. Special attention is being given to crossover theories [2], the central objective of which is to characterize the transition from the fluctuation-dominated regime (very close to the critical point) to the mean-field regime (far enough from the critical point) in a self-consistent, realistic way.

At the purely thermodynamic level, Griffiths and Wheeler's theory [3] was a valuable pioneering approach to the complete characterization of critical behavior. The theory is based on arguments and definitions of geometric character for the coexisting and critical surfaces in the space of thermodynamic field variables. A few simple postulates provide a general framework for understanding the thermodynamic behavior in the immediate vicinity of the wide variety of critical points in multicomponent systems. Although widely accepted, experimental checking of the predictions of the theory is currently a matter of interest. In that sense, liquid-liquid critical points for binary mixtures have been found among the most accessible (and appropriate) systems to be studied. In fact, a large amount of work has been devoted to them [4,5]. Griffiths and Wheeler developed various relations between second-order derivatives holding at the critical point for this type of transition such as the following:

$$\left(\frac{dT}{dp}\right)_c = T_c\left(\frac{\alpha_p}{C_p}\right)_c, \tag{1}$$

$$\left(\frac{dT}{dp}\right)_c^2 = T_c\left(\frac{\kappa_T}{C_p}\right)_c, \tag{2}$$

$$\left(\frac{dT}{dp}\right)_c^2 = T_c\left(\frac{\kappa_S}{C_v}\right)_c. \tag{3}$$

Note that all second-order derivatives in Eqs. (1)–(3) are mutually related via the critical temperature T_c and the slope of the critical line $(dT/dp)_c$, the latter of which appears to play a prominent role. For ordinary critical points—special points in the critical locus such as those where $(dT/dp)_c=0$ or $(dp/dT)_c=0$ are excluded—the isobaric heat capacity per unit volume, C_p, the isobaric thermal expansivity α_p, and the isothermal compressibility κ_T exhibit weak divergences to infinity at the critical point; on the other hand, the isochoric heat capacity per unit volume, C_v, and the isentropic compressibility κ_s remain finite [5]. The modern theory of critical phenomena is known to provide comprehensive information about the functional form of the critical part of thermodynamic properties. Thus, the linearization of the renormalization group equations around the critical point yields scaling laws with critical exponents and critical-amplitude ratios that depend on the universality class concerned. Like gas-liquid critical points of pure substances and Curie points of uniaxial ferromagnetic materials, liquid-liquid critical points belong to the so-called "universality class of the three-dimensional Ising model." Accordingly, the above-mentioned diverging quantities obey a power law of the following type in the immediate vicinity of the critical point:

$$Y = \frac{Y_0^{\pm}}{\alpha} t^{-\alpha}, \tag{4}$$

where Y can be C_p, α_p, or κ_T and $t=|T-T_c|/T_c$ denotes the reduced temperature. α is known as the critical exponent of the heat capacity and $Y_0^{\pm}$ are the critical amplitudes in the homogeneous (+) and heterogeneous (−) regions, respectively. A is normally used for the critical amplitude of C_p; in this work, we used B and C for α_p and κ_T, respectively. Calculations within the framework of the renormalization

TABLE I. Phase behavior of the studied systems. Critical compositions x_c, critical temperatures T_c (in kelvin), and slopes of the critical line $(dT/dp)_c$ (in mK bar^{-1}).

System	x_c	T_c This work	T_c Literature	$(dT/dp)_c$
NM-B_{OH}	0.582 [16]	290.86	290.31 [16] 291.11 [20]	4.6±0.7 [16]
NM-IB_{OH}	0.553 [16]	291.16	290.69 [16] 291.52 [21]	3.4±0.6 [16]
NE–*c*-C_6	0.453 [17]	296.62	296.62 [22] 296.96 [17]	15.0±0.1 [17]
DC-C_{10}	0.667 [16]	287.29	286.62 [23]	17.6±0.2 [16]
E_{OH}-C_{12}	0.687 [19]	285.64	285.64 [19] 285.8 [24]	23.1±1.2 [24]

group context gave $\alpha=0.1099\pm0.0007$ [6,7], which is one of the best known universal quantities as it has been determined also experimentally many times. In summary, based on Eq. (4), Eqs. (1) and (2) relate critical amplitudes via $(dT/dp)_c$; on the other hand, in Eq. (3), $(dT/dp)_c$ is related to the ratio of the limiting values of κ_s and C_v at the critical point.

Development following the work of Griffiths and Wheeler gave rise to a more general and rigorous formulation referred to as the principle of isomorphism of critical phenomena, a detailed description of which can be found elsewhere [5,8]. In the case of liquid-liquid phase transitions, the principle of isomorphism leads to three thermodynamic regions of markedly different behavior that are characterized by two system-dependent parameters $\tilde{t}_1$ and $\tilde{t}_2$. Then, the three regions are defined in terms of the reduced temperature in the following way: $t\ll\tilde{t}_2$, $\tilde{t}_2<t<\tilde{t}_1$, and $t\gg\tilde{t}_1$. The temperature interval $\tilde{t}_2<t<\tilde{t}_1$ is of great practical interest since it has been shown that the region $t\ll\tilde{t}_2$ is experimentally inaccessible [5]. In this context, it must be noted that Eqs. (1)–(4) are valid only in $t\ll\tilde{t}_2$, i.e., the immediate vicinity of the critical point; however, it is clear that the correct determination of $(dT/dp)_c$, critical amplitudes (A, B, and C), and limiting values ($\kappa_{s,c}$ and $C_{v,c}$) should result in the experimental verification of Eqs. (1)–(3). Current experimental methods [4,9] allow accurate $(dT/dp)_c$ values and reliable values for the critical amplitudes of the heat capacity to be obtained from $C_p(T)$ data. Direct measurements of $\alpha_p(T)$ in the critical region were formerly obtained using dilatometric techniques [10–12]; however, highly precise density measurements as a function of temperature, i.e., $\rho(T)$, are by now known to be a better choice. As regards Eq. (2), no appropriate experimen-

TABLE II. Fitting parameters of Eq. (5) and standard deviations s for studied critical mixtures. B, E, A^+, and A^- are in J K^{-1} cm^{-3}. The fixed value of α is 0.110.

Fit	B	E	A^+	A^-	α	s
			NM-B_{OH}			
(a_1)	1.36±0.01	1.02±0.18	0.0622±0.0007	0.1100±0.0007	Fixed	0.012
(a_2)	1.40±0.01	0.60±0.11	0.0606±0.0006		Fixed	0.005
(a_3)	1.39±0.13	0.60±0.17	0.061±0.005		0.11±0.01	0.005
			$T_c=290.898\pm0.002$ K; $A^+/A^-=0.565\pm0.005$			
			NM-IB_{OH}			
(a_1)	1.25±0.01	1.7±0.2	0.0721±0.0006	0.1290±0.0006	Fixed	0.02
(a_2)	1.29±0.01	0.77±0.11	0.0705±0.0005		Fixed	0.005
(a_3)	1.2±0.2	0.9±0.3	0.074±0.007		0.10±0.01	0.005
			$T_c=291.215\pm0.002$ K; $A^+/A^-=0.558\pm0.007$			
			NE–*c*-C_6			
(a_1)	1.32±0.01	−1.54±0.13	0.0253±0.0003	0.0488±0.0003	Fixed	0.01
(a_2)	1.25±0.01	0.30±0.14	0.0291±0.0003		Fixed	0.005
(a_3)	1.2±0.3	0.4±0.5	0.032±0.010		0.10±0.05	0.005
			$T_c=296.618\pm0.002$ K; $A^+/A^-=0.518\pm0.009$			
			DC-C_{10}			
(a_1)	1.48±0.01	−0.62±0.05	0.0235±0.0002	0.0459±0.0002	Fixed	0.006
(a_2)	1.45±0.01	−0.23±0.05	0.0249±0.0004		Fixed	0.004
(a_3)	1.50±0.11	−0.28±0.16	0.023±0.005		0.12±0.03	0.004
			$T_c=287.266\pm0.002$ K; $A^+/A^-=0.512\pm0.006$			
			E_{OH}-C_{12}			
(a_1)	1.71±0.01	0.88±0.04	0.0042±0.0002	0.0075±0.0002	Fixed	0.006
(a_2)	1.71±0.01	1.09±0.05	0.0044±0.0002		Fixed	0.004
(a_3)	1.70±0.02	1.07±0.07	0.0043±0.0007		0.10±0.02	0.004
			$T_c=285.660\pm0.002$ K; $A^+/A^-=0.56\pm0.03$			

tal method for determining κ_T providing useful information with a view to elucidating its critical behavior appears to exist. Equation (3) involves the isentropic compressibility, which can be obtained from sound speed analysis, and C_v, whose limiting value cannot be directly determined as it exhibits α-type diverging behavior in the experimentally accessible region ($\tilde{t}_2 < t < \tilde{t}_1$) [5,13,14]. It therefore appears that only Eq. (1) can be experimentally verified. Because the input quantities are $C_p(T)$, $\rho(T)$, and $(dT/dp)_c$, validating Eq. (1) entails verifying the thermodynamic consistency between the density and the heat capacity near the critical point. Substantial efforts have been made in this direction, the most noteworthy of which is that of Jacobs and Greer [15], who performed a comprehensive analysis of all reported data (five systems) and concluded that the critical amplitudes of C_p and ρ cannot be used to predict each other. In addition, they ascribed the problem to the above-described diverging behavior of C_v in the experimentally accessible region and the inherent difficulties in accurately determining the amplitude of the density anomaly. Also, eventual errors in any of the data sets used could be the cause of the discrepancies.

The above-mentioned facts clearly indicate that verification of Eq. (1) is still an open issue. Indeed, Jacobs and Greer suggested that further experiments would be worthwhile. Therefore, it is our purpose to provide accurate data in the vicinity of liquid-liquid critical points that could help to clarify this matter. Thus, $C_p(T)$ and $\rho(T)$ data in the critical region for five binary critical mixtures are presented and analyzed. The mixtures studied were nitromethane–1-butanol (NM-B_{OH}), nitromethane-isobutanol (NM-IB_{OH}), nitroethane-cyclohexane (NE–*c*-C_6), dimethyl carbonate–*n*-decane (DC-C_{10}), and ethanol–*n*-dodecane (E_{OH}-C_{12}). Their $(dT/dp)_c$ values were reported previously [16,17]. Although $C_p(T)$ and $\rho(T)$ for NM-B_{OH}, and $C_p(T)$ for NE–*c*-C6, were previously determined in our laboratory and reported [18], they are included here as reanalysis of the data is made. Also, although the choice of systems may seem accidental, all share some features, namely, (i) they are simple (not complex) mixtures that exhibit ordinary critical points of the (UCST, LCSP) type; and (ii) their critical temperatures lie just below ambient temperatures, which facilitates measurement. Checking for the thermodynamic consistency between C_p and ρ, i.e., Eq. (1), entailed careful analysis of the fitting procedures for $\rho(T)$ data. In addition, all relevant information concerning the universality of critical behavior that can be derived from C_p data was analyzed; α, the ratio of critical amplitudes of the heat capacity A^+/A^-, and the dimensionless parameter X, i.e., two-scale-factor universality, were determined and compared with their theoretical counterparts.

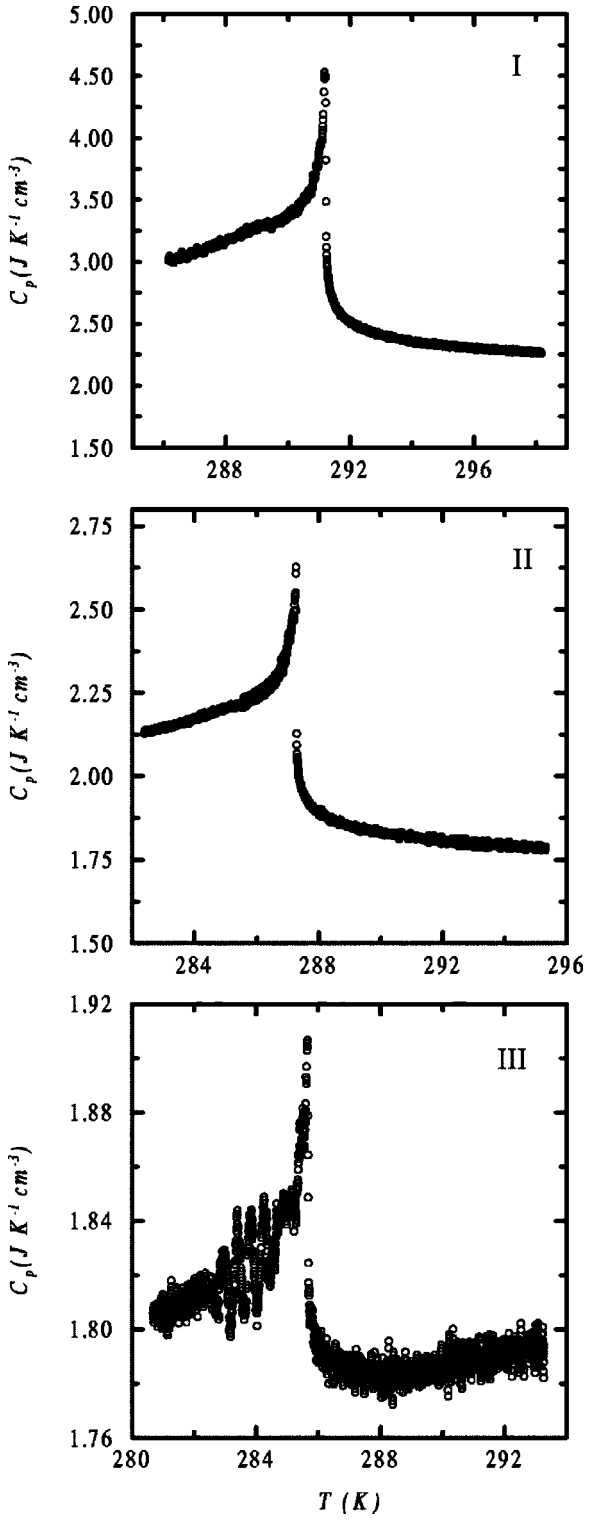

FIG. 1. Heat capacity per unit volume, C_p, in the critical region along an isobaric path for (I) NM-IB_{OH}, (II) DC-C_{10}, (III) E_{OH}-C_{12}.

II. EXPERIMENT

A. Sample preparation and chemicals

Dimethyl carbonate (over 99% pure), *n*-decane (over 99% pure), *n*-dodecane (over 99% pure), cyclohexane (over 99.9% pure), and isobutanol (over 99.4% pure) were obtained from Aldrich, while nitromethane (99% pure) and nitroethane (97% pure) were purchased from Fluka and ethanol (over 99.8% pure) from Merck. Dimethyl carbonate, isobutanol, nitromethane, nitroethane, and ethanol were dried over Fluka molecular sieves of 4 nm mesh size. All liquids were degassed prior to use. Critical mixtures were studied on the

TABLE III. Fitting parameters of Eq. (7) and standard deviations s for the studied critical mixtures. ρ_c, R_0, and R_1^+ are in g cm^{-3}. The fixed values of α and T_c are 0.110 and those contained in Table II, respectively.

Fit	ρ_c	R_0	R_1^+	α	s
		NM-B_{OH}			
(a_1)	0.954431±0.000003	−0.278±0.008	−0.025±0.005	Fixed	0.000004
(a_2)	0.954417±0.000004	−0.3197±0.0006			0.000006
		NM-IB_{OH}			
(a_1)	0.950205±0.000003	−0.285±0.007	−0.023±0.005	Fixed	0.000004
(a_2)	0.950193±0.000002	−0.3229±0.0005			0.000006
		NE–*c*-C_6			
(a_1)	0.863329±0.000003	−0.261±0.010	−0.041±0.006	Fixed	0.000005
(a_2)	0.863309±0.000003	−0.3289±0.0007			0.000007
		DC-C_{10}			
(a_1)	0.884927±0.000003	−0.253±0.009	−0.037±0.005	Fixed	0.000005
(a_2)	0.884907±0.000003	−0.3138±0.0006			0.000008
		E_{OH}-C_{12}			
(a_1)	0.765817±0.000003	−0.209±0.010	−0.010±0.006	Fixed	0.000004
(a_2)	0.765812±0.000002	−0.2258±0.0005			0.000004

basis of previously reported critical composition x_c values [16,17,19] that are listed in Table I. They were prepared by weighing using a Mettler AE-240 balance under a nitrogen atmosphere, and vigorously stirred prior to placement in the measuring cells. T_c was determined from turbidity measurements in our laboratory; the values thus obtained deviated randomly from the previously reported ones [16,17,19–24] (see Table I). These differences in T_c can be ascribed to the presence of impurities, which are known to affect the critical composition to a much lesser extent [25].

B. Equipment and procedures

Isobaric heat capacities per unit volume were obtained by using a Setaram micro DSC II calorimeter. This instrument and the underlying experimental methodology, Calvet scanning calorimetry, are described elsewhere [26]. The two measuring cells of the calorimeter were filled with 1 ml of sample and arranged in such a way that no vapor phase could contact the detection zone of the calorimeter. One of the cells held a reference substance (1-butanol in these measurements) and the other the critical mixture. Working in a down-scan mode, the calorimetric signal is the differential heat flow associated with a temperature decrease. Although the scanning rate can be as low as 0.001 K min^{-1}, we used 0.01 K min^{-1}, which afforded a signal reproducibility of ±0.02 mW; lower scanning rates give values that fall within the resolution limit of the calorimeter. Under these conditions, the reproducibility in C_p measurements was estimated to be ±0.0002 J K^{-1} cm^{-3}, somewhat poorer in the immediate vicinity of the critical point owing to the difficulties inherent in the experimentation in this region. The procedure was less reliable in the two-phase region as the calorimeter design precluded stirring of the mixture. The calorimetric signal was calibrated against two substances of known heat capacity (viz., 1-butanol and toluene) and the temperature was measured to within ±0.002 K with a platinum resistance thermometer. The ability of the calorimeter employed here to obtain C_p data in the liquid-liquid critical region was assessed in previous work [18]; reliable data were found to be obtained over a range of 0.01 K around the critical point. These conditions provided highly reliable values for the critical amplitudes and reasonably good ones for the critical exponent.

Densities in the one-phase region were obtained by using an Anton-Paar DSA-48 vibrating tube density meter. The whole experimental device is fully automated as described elsewhere [27]. Temperature was measured to ±0.002 K with a platinum resistance thermometer. The density meter was calibrated with water and *n*-octane as density standards. Correlation among data for the same run at different temperatures lay within ±0.000 005 g cm^{-3}.

III. RESULTS AND DISCUSSION

A. Heat capacity data: Universality

Verifying Eq. (1) entails avoiding or minimizing experimental sources of error in the input quantities. Thus, (i) one must ensure accuracy in primary measurements and (ii) raw data should be properly treated. As for (i), detailed information about purity, sample handling, and appropriateness of experimental techniques was given in the experimental section. As for (ii), objective fitting strategies must be used with a view to obtaining reliable information from the data; as will be shown in detail in Sec. III B, this was the "critical" requirement with densities. This section is devoted to C_p data.

Figure 1 shows the lambda C_p curves for NM-IB_{OH}, DC-C_{10}, and E_{OH}-C_{12}. The temperature ranges studied were

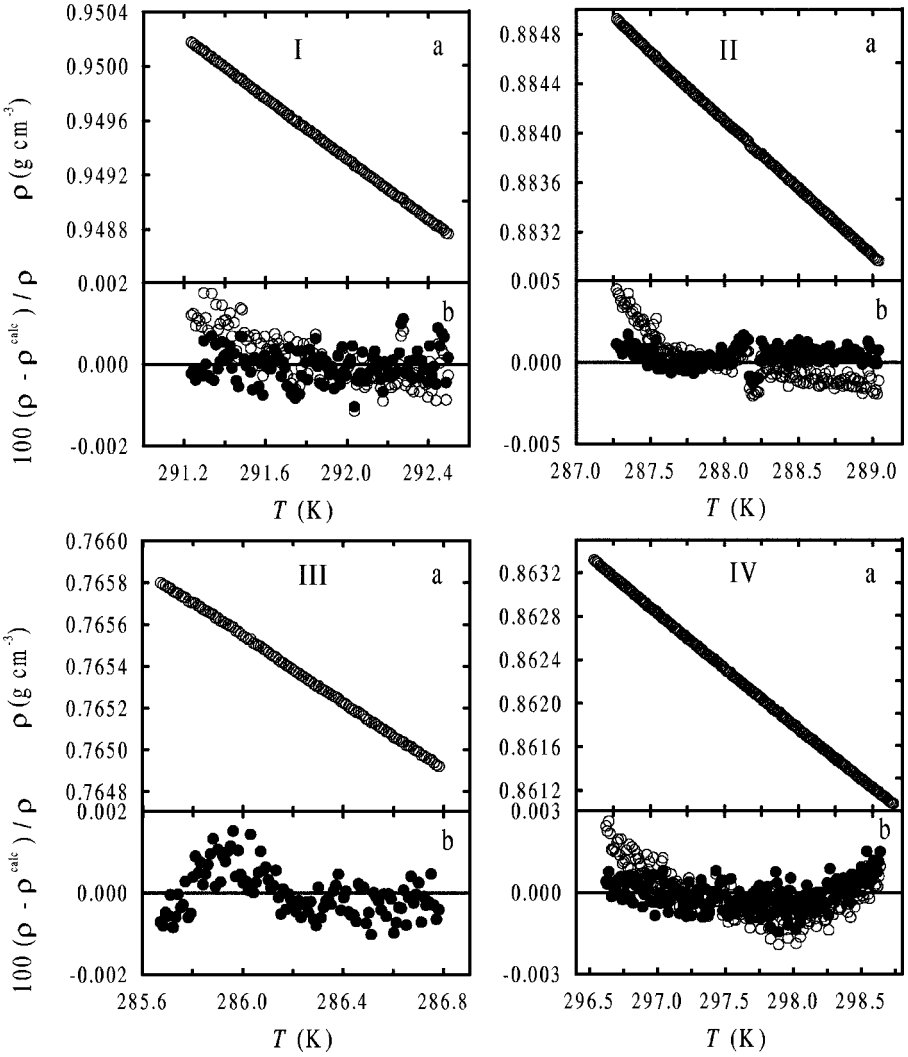

FIG. 2. (a) Density ρ in the one-phase critical region along an isobaric path; data about 1 K above the critical temperature. (b) Residuals calculated from Eq. (7) with (●) fitting approach (a_1) and (○) fitting approach (a_2). (I) NM-IB_{OH}, (II) DC-C_{10}, (III) E_{OH}-C_{12}, and (IV) NE–*c*-C_6.

286.15-298.15 K, 282.15-295.15 K, and 280.15-293.15 K, respectively. As can be seen, NM-IB_{OH} exhibits the largest anomaly; on the other hand, the anomaly in E_{OH}-C_{12} is so small that it lies within the detection limit of the calorimeter. Data were fitted to

$$C_p = B + Et + \frac{A^{\pm}}{\alpha} t^{-\alpha}. \tag{5}$$

Equation (5) contains a pure asymptotic power-law term—correction-to-scaling terms were omitted as explained previously [18]—and a regular contribution (a linear function of the reduced temperature). Fitting was done in three different ways. In approach (a_1), all data (both in the homogeneous and in the heterogeneous region) were included, A^+, A^-, T_c, B, and E being the fitting parameters and α fixed to its accepted value. In (a_2) and (a_3), only data in the homogeneous region were used and T_c was fixed to the value obtained in approach (a_1). Approach (a_2) involved the same procedure as (a_1) and approach (a_3) included α among the fitting parameters. Approach (a_3) provides experimental values for α, however, it results in correlation between α and A^+ and, hence, in potential errors. Because data in the heterogeneous region are less reliable, approach (a_2) seemingly provides the best A^+ values; however, (a_1) gives more information as it allows the universality of the ratio A^+/A^- (its renormalization group value is 0.537 ± 0.019 [28]) to be checked. The values of the coefficients and the standard deviations of the fits are shown in Table II. The results warrant four immediate comments. First, the T_c values in Table II are consistent with those obtained from turbidity measurements (Table I). Second, the α values coincide with the accepted value to within ±0.01. Third, these results appear to confirm the universality of A^+/A^- as they are quite consistent with the renormalization group value (deviations between the experimental and the renormalization group value are around ±0.03); thus, it can be concluded that, even in the absence of stirring, our calorimeter provides reasonably reliable data in the two-phase region. Finally, two-scale-factor universality states the existence of a universal dimensionless parameter X (its renormalization group value is $0.019\,66 \pm 0.000\,17$ [29]) relating the amplitude of the heat capacity in the homogeneous region to that of the correlation length ξ_0^+ via the Boltzmann constant k_B:

$$X = \frac{A^+(\xi_0^+)^3}{k_B}. \tag{6}$$

Based on Eq. (6), a large ξ_0^+ value must be the origin of the small C_p anomaly in E_{OH}-C_{12}. The reported value for this mixture as obtained from light scattering experiments is 0.34 ± 0.01 nm [19]; substitution of our A^+ value in Eq. (6) gives 0.39 ± 0.02 nm. The relatively large uncertainty in the direct determination of ξ_0^+ (e.g., the reported ξ_0^+ values for methanol + cyclohexane, which is considered a reference system since its ξ_0^+ value has been determined in different laboratories, range from 0.32 to 0.39 nm) makes the results consistent with Eq. (6) and reveals the reliability of the calorimetric data in spite of the small C_p anomaly of E_{OH}-C_{12}.

B. Density data: Thermodynamic consistency between C_p and ρ

The high consistency of the information derived from C_p data lies in the various proofs of universality and makes them suitable for testing Eq. (1). The determination of the α_p anomaly is rather complicated as it relies on $\rho(T)$, which exhibits a small anomaly. The mere observation of Fig. 2, which shows densities in the homogeneous region for all the systems except NM-B_{OH}, clarifies this point. The temperature ranges covered were from T_c to 299.15 K for NM-IB_{OH}, 303.15 K for NE–*c*-C_6, 295.65 K for DC-C_{10}, and 291.91 K for E_{OH}-C_{12}. The following equation for $\rho(T)$, based on that for the α_p critical anomaly [Eq. (4)], was used:

$$\rho = \rho_c + R_0 t + R_1^+ t^{1-\alpha}. \tag{7}$$

Equation (7) includes a regular part (a linear function of t) and the critical contribution (last term on the right-hand side). A quadratic form for the regular contribution and/or first correction-to-scaling term for the critical one have been considered in fitting $\rho(T)$ data [15]. Based on the small magnitude of the density anomaly, we thought it important not to include too many parameters in order to avoid mutual correlation. Thus, we chose Eq. (7) as it is the simplest realistic one; however, it must be ensured that (i) the assumption of a linear regular contribution is appropriate and (ii) no correction-to-scaling terms are needed. A preliminary study on previously measured density data in our laboratory for pure liquids and mixtures far away from critical points revealed that ρ varies linearly with T within the experimental detection limits ($\pm 0.000\,005$ g cm^{-3}, as described in the experimental section) over a range not much wider than 3 K. Therefore, if only data within such a range above the critical temperature are included in the fitting, requirements (i) and (ii) will be satisfied and reliable R_1^+ values obtained as a result. Two types of fits of data within (T_c, T_c+3)K including (a_1) regular and critical terms and (a_2) regular terms alone were used. In both cases, T_c was fixed to the values listed in Table II, whereas α was fixed to its accepted value in (a_1). The final results for the parameters and the standard deviations using both approaches are given in Table III. As can be seen, fitting approach (a_1) did not significantly reduce the standard deviation; however, plots (b) in Fig. 2 clearly illustrate the improvement in the immediate vicinity of T_c. The only exception is E_{OH}-C_{12}, where its small density anomaly is undetectable within the resolution limits of the measurements (as can be seen in Fig. 2, the residuals for both approaches are indistinguishable); this is consistent with the findings of previous work [30], where similar density values were reported. Therefore, the R_1^+ value of Table III for this system is not statistically significant.

TABLE IV. R_1^+ values in g cm^{-3} for the studied critical mixtures as obtained from Eqs. (7) and (9).

System	R_1^+ Eq. (7)	R_1^+ Eq. (9)
NM-B_{OH}	-0.025 ± 0.005	-0.027 ± 0.005
NM-IB_{OH}	-0.023 ± 0.005	-0.023 ± 0.005
NE–*c*-C_6	-0.041 ± 0.006	-0.039 ± 0.002
DC-C_{10}	-0.037 ± 0.005	-0.040 ± 0.002

Once both $C_p(T)$ and $\rho(T)$ data were carefully treated, the thermodynamic consistency between them was readily examined. The critical amplitude of α_p is related to R_1^+ by

$$B^+ = -\frac{\alpha(1-\alpha)R_1^+}{\rho_c T_c}. \tag{8}$$

Therefore, Eq. (1) can be expressed in terms of the critical amplitudes [Eqs. (6) and (7)] as

$$R_1^+ = \pm \frac{\rho_c (dT/dp)_c}{\alpha(1-\alpha)} A^+, \tag{9}$$

where the plus sign corresponds to lower consolute points and the minus sign to upper consolute points (this work). Table IV shows the R_1^+ values obtained from the density data of Table III and those obtained by using $(dT/dp)_c$ (Table I) and A^+ [Table II, approach (a_2)] values in Eq. (9). The good agreement within the quoted experimental uncertainties constitutes a proof of the thermodynamic consistency between the density and the heat capacity near the critical point. The consistency between these two sets of values testifies to the soundness of the experimental techniques and fitting procedures used. In particular, the key step for success is the strategy for the determination of R_1^+, which otherwise provides an *a posteriori* confirmation of the correctness of the fitting approach used.

IV. CONCLUSION

The main goal of this experimental study was to verify the thermodynamic consistency between C_p and ρ near the liquid-liquid critical point as predicted from the Griffiths-Wheeler theory. The information derived from C_p data was found to be highly reliable—the various proofs of universality confirmed this point—implying that the problem is reduced to ρ data. In particular, the fitting strategy for determining the amplitude of the density anomaly appeared to be the key factor in checking the thermodynamic consistency between both properties. The possibility of determining the amplitude of the anomaly in ρ accurately suggests further tests of thermodynamic consistency near liquid-liquid critical points.

[1] J. J. Binney, N. J. Dowrick, A. J. Fisher, and M. E. J. Newman, *The Theory of Critical Phenomena: An Introduction to the Renormalization Group*, 4th ed. (Clarendon Press, Oxford, 1992), Vol. 1, Chap. 1, p. 1.
[2] A. Kostrowicka Wyczalkowska, J. V. Sengers, and M. A. Anisimov, Physica A **334**, 482 (2004).
[3] R. B. Griffiths and J. C. Wheeler, Phys. Rev. A **2**, 1047 (1970).
[4] A. Kumar, H. R. Krishnamurthy, and E. S. R. Gopal, Phys. Rep. **98**, 57 (1983).
[5] M. A. Anisimov, in *Critical Phenomena in Liquids and Liquid Crystals*, 1st English ed. (Gordon and Breach, Philadelphia, 1991), Vol. 1, Chap. 3, p. 63.
[6] P. Butera and M. Comi, Phys. Rev. B **58**, 11 552 (1998).
[7] M. Campostrini, A. Pelissetto, P. Rossi, and E. Vicari, Phys. Rev. E **60**, 3526 (1999).
[8] M. A. Anisimov, E. E. Gorodetskii, V. D. Kulikov, and J. V. Sengers, Phys. Rev. E **51**, 1199 (1995).
[9] J. V. Sengers and J. M. H. Levelt-Sengers, in *Progress in Liquid Physics*, 1st ed., edited by Clive A. Croxton (Wiley & Sons, New York, 1978), Vol. 1, Chap. 4, p. 103.
[10] K. Govindarajan, B. Viswanathan, and E. S. R. Gopal, J. Chem. Thermodyn. **5**, 73 (1973).
[11] E. S. R. Gopal, R. Rachamandra, M. V. Lele, P. Chandrasekhar, and N. Nagarajan, J. Indian Inst. Sci. **56**, 193 (1974).
[12] B. A. Scheibner, C. M. Sorensen, D. T. Jacobs, R. C. Mockler, and J. O'Sullivan, Chem. Phys. **31**, 209 (1978).
[13] M. A. Anisimov, A. V. Voronel, and T. M. Ovodova, Sov. Phys. JETP **34**, 536 (1972).
[14] M. A. Anisimov, A. T. Berestov, V. P. Voronov, Y. F. Kiyachenko, B. A. Koval'chuk, V. M. Malyshev, and V. A. Smirnov, Sov. Phys. JETP **49**, 844 (1979).
[15] D. T. Jacobs and S. C. Greer, Phys. Rev. E **54**, 5358 (1996).
[16] L. P. N. Rebelo, V. Najdanovic-Visak, Z. P. Visak, M. Nunes da Ponte, J. Troncoso, C. A. Cerdeiriña, and L. Romaní, Phys. Chem. Chem. Phys. **4**, 2251 (2002).
[17] J. Thoen, J. Hamelin, and T. K. Bose, Phys. Rev. E **53**, 6264 (1996).
[18] C. A. Cerdeiriña, J. Troncoso, E. Carballo, and L. Romaní, Phys. Rev. E **66**, 031507 (2002).
[19] D. Dürr, S. Z. Mirzaev, and U. Kaatze, J. Phys. Chem. A **104**, 8855 (2000).
[20] J. M. Sorensen and W. Arlt, *Liquid-Liquid Equilibria Data Collection*, 1st edition (Dechema, Frankfurt, 1979), Vol. 1, Chap. 1, p. 30.
[21] A. Milewska and J. Szydlowski, J. Chem. Eng. Data **44**, 505 (1999).
[22] H. L. Clever, Q. R. Pirkle, B. J. Allen, and E. Derrick, J. Chem. Eng. Data **17**, 31 (1972).
[23] J. A. González, I. García, J. C. Cobos, and C. Casanova, J. Chem. Eng. Data **36**, 162 (1991).
[24] U. Dahlmann and G. M. Schneider, J. Chem. Thermodyn. **21**, 997 (1989).
[25] D. T. Jacobs, J. Chem. Phys. **91**, 560 (1989).
[26] C. A. Cerdeiriña, J. A. Míguez, E. Carballo, C. A. Tovar, E. de la Puente, and L. Romaní, Thermochim. Acta **347**, 37 (2000).
[27] J. Troncoso, E. Carballo, C. A. Cerdeiriña, D. González, and L. Romaní, J. Chem. Eng. Data **45**, 594 (2000).
[28] R. Guida and J. Zinn-Justin, J. Phys. A **31**, 8103 (1998).
[29] C. Berviller, Phys. Rev. B **21**, 5427 (1980).
[30] K. Orzechovski, J. Chem. Soc., Faraday Trans. **90**, 2757 (1994).